



Detection of Quiescent Radioresistant Epithelial Progenitors in the Adult Thymus

Maude Dumont-Lagacé^{1,2}, Hervé Gerbe¹, Tariq Daouda^{1,3}, Jean-Philippe Laverdure¹, Sylvie Brochu¹, Sébastien Lemieux^{1,4}, Étienne Gagnon^{1,5} and Claude Perreault^{1,2*}

¹Institute for Research in Immunology and Cancer, Montreal, QC, Canada, ²Department of Medicine, Université de Montréal, Montréal, QC, Canada, ³Department of Biochemistry, Université de Montréal, Montréal, QC, Canada, ⁴Department of Informatics and Operational Research, Université de Montréal, Montréal, QC, Canada, ⁵Department of Microbiology, Infectiology and Immunology, Université de Montréal, Montréal, QC, Canada

OPEN ACCESS

Edited by:

Nick Gascoigne,
National University of Singapore,
Singapore

Reviewed by:

Ann Chidgey,
Monash University, Australia
David L. Wiest,
Fox Chase Cancer Center,
United States

*Correspondence:

Claude Perreault
claude.perreault@umontreal.ca

Specialty section:

This article was submitted
to T Cell Biology,
a section of the journal
Frontiers in Immunology

Received: 29 September 2017

Accepted: 21 November 2017

Published: 05 December 2017

Citation:

Dumont-Lagacé M, Gerbe H,
Daouda T, Laverdure J-P, Brochu S,
Lemieux S, Gagnon É and
Perreault C (2017) Detection of
Quiescent Radioresistant Epithelial
Progenitors in the Adult Thymus.
Front. Immunol. 8:1717.
doi: 10.3389/fimmu.2017.01717

Thymic aging precedes that of other organs and is initiated by the gradual loss of thymic epithelial cells (TECs). Based on *in vitro* culture and transplantation assays, recent studies have reported on the presence of thymic epithelial progenitor cells (TEPCs) in young adult mice. However, the physiological role and properties of TEPC populations reported to date remain unclear. Using an *in vivo* label-retention assay, we previously identified a population of quiescent but non-senescent TECs. The goals of this study were therefore (i) to evaluate the contribution of these quiescent TECs to thymic regeneration following irradiation-induced acute thymic injury and (ii) to characterize their phenotypic and molecular profiles using flow cytometry, immunohistology, and transcriptome sequencing. We report that while UEA1⁺ cells cycle the most in steady state, they are greatly affected by irradiation, leading to cell loss and proliferative arrest following acute thymic involution. On the opposite, the UEA1⁻ subset of quiescent TECs is radioresistant and proliferate *in situ* following acute thymic involution, thereby contributing to thymic regeneration in 28- to 30-week-old mice. UEA1⁻ quiescent TECs display an undifferentiated phenotype (co-expression of K8 and K5 cytokeratins) and express high levels of genes that regulate stem cell activity in different tissues (e.g., *Podxl* and *Ptprz1*). In addition, two features suggest that UEA1⁻ quiescent TECs occupy discrete stromal niches: (i) their preferential location in clusters adjacent to the cortico-medullary junction and (ii) their high expression of genes involved in cross talk with mesenchymal cells. The ability of UEA1⁻ quiescent TECs to participate to TEC regeneration qualifies them as *in vivo* progenitor cells particularly relevant in the context of regeneration following acute thymic injury.

Keywords: thymic epithelial cells, stem cells, thymic regeneration, label-retention assay, transcriptomics

INTRODUCTION

In all vertebrates, the thymus is the sole organ that can generate functional classic (TCRαβ⁺) T lymphocytes (1). Thymic epithelial cells (TECs) are responsible for the unique properties of the thymus: they orchestrate each steps of T-cell development and regulate thymic output (2, 3). In adults, the production of naive T cells gradually decreases with age, a decline caused by the

loss of TECs, which entails a reduction in the TCR repertoire diversity (4). It was therefore somewhat surprising to realize that TECs are not post-mitotic cells and that they retain extensive regenerative capacities even in adults (5, 6). Indeed, medullary TECs (mTECs), and to a lesser extent cortical TECs (cTECs), turnover rapidly in healthy animals (6–8). In addition, the thymus has the ability to regenerate following various acute injuries induced by stress, infection, sublethal irradiation, or pregnancy (9–13). However, more severe injuries inflicted by chemotherapy or radiation therapy can overwhelm the regenerative potential of the thymic epithelium and lead to prolonged immune deficiency (14, 15). Since tissue repair is usually driven by stem-progenitor cells, identification of thymic epithelial progenitor cells (TEPCs) responding to thymic injury should provide key insights into the mechanisms of thymic regeneration.

Various stem cells including hematopoietic stem cells (16), muscle satellite cells (17), and hair follicle stem cells (18) are quiescent in steady-state conditions. We therefore hypothesized that isolation of non-dividing TECs might enable us to enrich for a population of quiescent TEPCs. To this end, we used an *in vivo* label-retaining cell (LRC) assay in which cells expressed a histone 2B-GFP fusion protein (H2B-GFP) inducible under the control of the reverse tetracycline-controlled transactivator (rtTA). Using this approach, we have previously shown that in adult mice, the UEA1⁻ TECs (mostly cTECs) contain more LRCs than UEA1⁺ TECs (mTECs), and that non-dividing UEA1⁻ LRCs were quiescent rather than senescent (7). Indeed, UEA1⁻ LRCs expressed low levels of senescence-associated transcripts (*p16INK4*, *p19ARF*, and *Serpine1*) and high levels of transcripts instrumental to TEC regeneration (*Bmi1*, *Trp63*, and *Wnt4*).

Previous studies have shown that transplantation can activate stem cell behavior in cells that do not act as stem cells in normal situation (19). The goal of this study was therefore to evaluate the contribution of endogenous (untransplanted) LRCs to thymus regeneration and to gain further insights into their *in situ* spatial distribution and molecular attributes. In addition, we wished to evaluate the proliferative activity of TEC subsets in two settings: steady-state conditions vs thymic regeneration following acute injury. We report that while the non-quiescent UEA1⁺ TECs cycle more actively than other TEC subsets under steady-state conditions, they are greatly affected by irradiation, leading to cell loss and a significant decrease in their proliferative activity. On the contrary, while other TEC subsets (i.e., UEA1⁻ TECs and quiescent UEA1⁺ TECs) proliferate modestly in physiological settings, they did not suffer cell loss from radiations. Interestingly, one particular TEC subset, the UEA1⁻ LRCs, increased its proliferation during the regenerative phase following thymic injury induced by irradiation, showing that it contains quiescent radioresistant TEPCs activated during tissue repair.

Using immunofluorescence analysis, we observed that most LRCs co-express both K8 and K5 cytokeratins, an undifferentiated phenotype observed in embryonic TEPCs, and are located near the cortico-medullary junction (CMJ) where they form cell clusters. Furthermore, the transcriptomic profile of UEA1⁻ LRCs showed low expression of genes implicated in interactions with thymocytes and high expression of genes involved in interactions with stromal cells and extracellular matrix (ECM). These

results suggest that UEA1⁻ LRCs are localized in specialized niches which are instrumental in the regulation of TEPCs activity. Finally, we identified six potential regulators of quiescent radioresistant TEPCs that are known to either regulate stem cell activity through niche interactions in other tissues (*Podxl*, *Ptprz1*, and *Angpt1*) or whose stromal cell ligands regulate thymic output (*Tgfrb3*, *Fzd4*, and *Ar*).

MATERIALS AND METHODS

Mice

B6.Cg-Gt(*ROSA*)26Sor^{tm1(rtTA^{M2})ae}/J and STOCK Tg(tetO-HIST1H2B)/GFP47Efu/J mice purchased from The Jackson Laboratory (Bar Harbor) were bred and housed under specific-pathogen-free conditions in sterile ventilated racks at the Institute for Research in Immunology and Cancer. For H2B-GFP pulse-chase experiments, doxycycline was incorporated in food (2 g/kg) (Harlan Laboratories), or in drinking water (2 mg/ml of doxycycline supplemented with 5% sucrose) for a 6-week pulse period. Only female mice were analyzed in this study. All procedures were in accordance with the Canadian Council on Animal Care guidelines and approved by the Comité de Déontologie et Expérimentation Animale de l'Université de Montréal.

Thymic Stroma Digestion

Enrichment of thymic stromal cells was performed as previously described (20). Briefly, thymic tissue was cut into small fragments and thymocytes released were removed from the supernatant. Stromal fragments were then digested at 37°C using a solution of 0.01% Liberase TM (Roche Applied Science) and 0.1% DNase-1 (Sigma-Aldrich) in RPMI-1640 with HEPES (Gibco) for three periods of 15 min. After the second incubation, cells released in the supernatant were removed and placed on ice and new fresh enzyme solution was added to the remaining fragments. The stromal cells in suspension were filtered before staining and analysis.

Flow Cytometry and Immunofluorescence Microscopy

The list of antibodies is provided in Supplementary Experimental Procedures (Table S1 in Supplementary Material). Viability of cells was assessed using 7-AAD or Propidium Iodide (BD Biosciences). Cell sorting was performed using three laser FACSAria (BD Biosciences) or analyzed on a three laser LSR II (BD Biosciences) using FACSDiva software (BD Biosciences).

Immunofluorescence microscopy was performed on cryosections of female thymi extracted after a 16-week chase period. Appropriate isotype and negative controls were included in all experiments. For detection of immunofluorescence, slices were examined using the Nanozoomer 2.0-HT from Hamamatsu, and NDPscan software (Hamamatsu) was used for image analysis. Quantification of K5⁺, K8⁺, or K5⁺K8⁺ surface area was performed using ImageJ, and LRCs were identified as having fluorescence intensity four times that of the cells in the negative controls with the maximal fluorescence intensity (see Figure S1 in Supplementary Material).

Thymic Injury and Bromodeoxyuridine (BrdU) Incorporation

Female mice at 16 weeks of chase were irradiated at a sublethal dose of 550 cGy to induce thymic involution (day 0). Four days after the irradiation, intraperitoneal injections of BrdU (1.5 mg per injection) were given daily for 3 days (days 4–6). At day 7, the mice were sacrificed, and the thymus was extracted for analysis. For control mice, the same procedure was performed without irradiation, at the end of the chase period.

Statistical Analyses

Unless stated otherwise, results are expressed as means \pm SD, and statistical significance was assessed using unpaired two-tailed Student's *t*-test. We verified the goodness of fit to the Poisson distribution using maximum likelihood to assess the statistical significance of dispersion index, calculated from the location of LRCs on thymic slices.

RNA Sequencing

We analyzed the transcriptome of two populations of TECs: UEA1⁻ LRCs (GFP^{hi}) and UEA1⁻ NonLRCs (GFP⁻) from females after a 6-week pulse period and a 16-week chase period. We obtained one biological replicates of each TEC population from a pool of 11 mice to get a minimum of 10⁴ cells per sample. Total RNA was isolated using Trizol™ as recommended by the manufacturer (Invitrogen), and then further purified using RNeasy Micro columns (Qiagen). Sample quality was assessed using Bioanalyzer RNA Pico chips (Agilent). Transcriptome libraries were made using the TruSeq RNA Sample Prep Kit (v2) (Illumina) following the manufacturer's protocols. Library generation was then assessed using a Bioanalyzer platform (Agilent) and Illumina MiSeq-QC run. Then, sequencing was done using Illumina HiSeq2000 and TruSeq SBS v3 chemistry at the Institute for Research in Immunology and Cancer's Genomics Platform. Cluster density was targeted at around 800 k clusters/mm². Data were mapped to the *Mus musculus* (mm10) reference genome using the ELANDv2 alignment tool from the CASAVA 1.8.2 software (Illumina). RNA-Seq data have been deposited in GEO archives under accession number GSE94642 and are displayed in Table S3 in Supplementary Material.¹ Analyses of RNA-sequencing data were performed using the publicly available statistical software package "R."² To remove genes that were lowly expressed in our analysis, we considered only genes that had a relative expression higher than 1 RPKM in at least one sample. Enrichment of biological functions were performed using the Gene Functional Annotation tool from DAVID bioinformatics resources³ [version 6.8 (21, 22)], and reduction of redundancy through semantic similarity was performed using REVIGO web-based tool for gene ontology (GO) analysis (23).

RNA-Seq data for Sca1⁺ mesenchymal cells and for UEA1⁺ TECs from female mice were extracted from Patenaude and Perreault (24) and Dumont-Lagacé et al. (25), respectively. Data

can be found under GEO accession numbers GSE60101 and GSE66873.

RESULTS

Experimental Model

The ROSA26-rtTA;TetO-H2B-GFP transgenic mouse model allows the identification of slow-cycling cells through label retention in a pulse-chase assay (18, 26, 27). The reverse tetracycline-controlled transactivator (rtTA) allows doxycycline-inducible expression of H2B-GFP in all cells. The proliferative history of cells can therefore be evaluated by measuring the fluorescence intensity of the remaining H2B-GFP over time. After pulse, the H2B-GFP fluorescence of non-dividing cells remains above negative control (H2B-GFP⁺ WT, see Figure S2 in Supplementary Material) for at least 6 months after doxycycline withdrawal, and at least five cell divisions are required for H2B-GFP to become undistinguishable from negative control by flow cytometry (28, 29).

In adults, female TECs proliferate more actively than male TECs, mostly because of the inhibitory effect of androgens (7, 25). Therefore, it is preferable to analyze TECs from both sexes separately. In this study, we analyzed only female mice from which TECs (EpCAM⁺CD45⁻) were divided into two populations based on UEA1 expression (Figure S2A in Supplementary Material). As UEA1⁺ TECs derive from an undifferentiated UEA1⁻ progenitor (30, 31), we analyzed UEA1⁺ and UEA1⁻ TECs, reasoning that progenitor cells should be enriched in the UEA1⁻ compartment. The 6-weeks doxycycline treatment was initiated at 4–6 weeks of age (pulse) and was followed by a chase period of 16 weeks (26–28 weeks of age at time of analysis). We defined two fluorescence thresholds for experimental purposes: (i) GFP^{hi} cells, with the fluorescence intensity of LRCs, that is, cells that did not divide during the 16 weeks of chase, taking into account the 24-day half-life of the H2B-GFP protein (Figure S2B in Supplementary Material) (32) and (ii) GFP^{int} cells, with a fluorescence intensity above the negative control but below the GFP^{hi} threshold. The fluorescence intensity of LRCs (GFP^{hi}) after the chase period was at least four times higher than the threshold that distinguishes GFP⁻ from GFP^{int} cells (Figure S2B in Supplementary Material). This means that at the term of the chase period, an LRC would become GFP⁻ after a minimum of three cell divisions (eightfold GFP dilution). Henceforth, in flow cytometry analyses, the term LRC will only be used to refer to GFP^{hi} cells.

Whereas the initial 6-week pulse enabled the homogenous and high GFP labeling of >75% of TECs, only a small proportion of TECs remains GFP^{hi} (i.e., LRCs) after 16 weeks of chase: 5.5% of UEA1⁻ TECs and 1.8% of UEA1⁺ (Figures S2B,C in Supplementary Material). Approximately 60% of LRCs were UEA1⁻, even if only one-third of TECs are UEA1⁻ (Figure S2C in Supplementary Material) This is consistent with previous studies showing that mTECs (UEA1⁺) turnover more rapidly than cTECs (UEA1⁻) in adult mice (7, 25).

Most LRCs Cluster in Proximity to the CMJ

Using immunofluorescence microscopy, we first investigated the location and phenotype of LRC TECs after the 16-weeks chase

¹<https://www.ncbi.nlm.nih.gov/geo/query/acc.cgi?acc=GSE94642>.

²<http://www.r-project.org/>.

³<https://david.ncifcrf.gov/>.

period. In tissue sections, we defined TECs as cells expressing cytokeratin 8 (K8) and/or cytokeratin 5 (K5) and LRCs as cells having a fluorescence intensity four times greater than the cells with the maximal signal in the negative control (see Figure S1 in Supplementary Material). Labeling with antibodies against K8 and K5, respectively, defined cortical and medullary regions of the thymus (Figure 1A). We evaluated the number of LRCs in each TEC subset (K5⁺, K8⁺, and K5⁺K8⁺) and the relative surface area covered by individual subsets. The salient finding was that LRCs were depleted from the K8⁺ and K5⁺ population and significantly enriched in the K5⁺K8⁺ population (Figures 1B,C). Indeed, while K5⁺K8⁺ TECs only occupy 26% of the surface area, they contain 63% of the LRCs. Since expression of both K5 and K8 is typical of TEPCs at embryonic day E12.0 (33) and becomes rare in the adult thymus, we conclude that most LRCs have a phenotype typical of undifferentiated TEPCs.

We next counted the number of LRCs found in each region of the thymus: cortex, medulla, and cortico-medullary region (CMR). The CMR was defined as the area spanning 100 μ m on either side of the CMJ delimited by K5 (Figure S3A in Supplementary Material). Notably, more than half of LRCs (53.6%) were found in the CMR (Figure 1D). We also observed that many LRCs formed clusters, while large regions of the stroma were devoid of any LRCs (Figure 2A). To quantify this phenomenon, we separated thymic slices in 40–50 non-overlapping sections of equal surface area (Figure S3B in Supplementary Material) and counted the number of LRCs expressing at least one cytokeratin in each section. While individual sections contained an average of 16 LRCs, we observed that half (52.4%) of LRCs were located within sections containing >32 LRCs, a few even containing more than 100 LRCs each (Figure 2B). However, only 12.9% of all areas contained such clusters (in green, Figure 2B). To rule out the possibility that this distribution was random, we compared it with a Poisson distribution created with the LRCs distribution's average ($\lambda = 16.11236$) and containing the same number of values ($k = 178$) and confirmed that the distributions were significantly different ($p < 2.2 \times 10^{-16}$; goodness of fit). We then calculated the dispersion index associated with LRCs' distribution. In a context where the positions of events would be completely independent of one another, the dispersion index would be equal to 1, as represented by the Poisson distribution. In a non-randomly dispersed dataset, a dispersion index > 1 means that the events tend to group together, leaving empty spaces in-between clusters of events. On the opposite, a dispersion index < 1 corresponds to a pattern of organization more regular than the randomness associated with the Poisson distribution. The dispersion index of LRCs in thymic slices was 34.81, showing that LRCs were grouped in clusters (Figure 2B). Together, these results show that most LRCs present an undifferentiated phenotype and are found in clusters at the CMJ, suggesting the existence of a specialized microenvironment (niche) for these quiescent cells.

UEA1⁻ LRCs Increase Their Proliferation Rate following Acute Thymic Injury

We studied TEC proliferation using BrdU incorporation. It must be reminded that upon division, the H2B-GFP content in LRCs

decreases by 50% in the daughter cells, and therefore LRCs' progeny might become GFP^{int}. Consequently, we reasoned that cells derived from LRCs which had undergone one or two cell divisions would be BrdU⁺ and either GFP^{hi} or GFP^{int} (regrouped under GFP⁺ in Figure 3). This definition may slightly underestimate the LRC progeny because after three cell divisions, the LRC progeny would become GFP⁻ in tissue sections (through dilution). To minimize this bias, we allowed BrdU incorporation during only a short pulse period of three days, starting at the end of the 16-week H2B-GFP chase period. Thymi were then extracted on the following day and analyzed for BrdU incorporation. Under steady-state conditions, most BrdU⁺ TECs derived from UEA1⁺ NonLRCs (labeled GFP⁻ in Figure 3). This is consistent with previous reports that mTECs (UEA1⁺) proliferate more extensively than other TEC subsets in adult mice (7, 25).

We next assessed TEC regeneration following acute thymic injury, using the well characterized model of sublethal-total body irradiation (SL-TBI) without hematopoietic rescue. SL-TBI induces an acute thymic involution and thymic weight reaches a nadir 3 days after irradiation (7, 34, 35). This involution phase is followed by a regenerative phase as thymic cellularity returns to normal levels within a few weeks. At the end of the H2B-GFP chase period (i.e., at 26–28 weeks of age), mice were irradiated on “day 0” with a sublethal dose of 550 cGy (Figure 3B). As expected, we observed global thymic hypocellularity 7 days after SL-TBI, followed by regeneration between day 7 and 14 (Figure 3C). Consistent with the notion that actively cycling cells are particularly sensitive to irradiation (36), the decrease in TEC numbers on day 7 post-SL-TBI was due exclusively to the loss of UEA1⁺GFP⁻ NonLRCs (Figure 3D).

To monitor TEC proliferation at the onset of thymic regeneration, mice were given daily intraperitoneal injections of BrdU from day 4 to day 6 after SL-TBI (Figure 3B), i.e., during the first days of thymic regrowth (11, 34, 35), and the percentage of BrdU⁺ cells was assessed at day 7 (Figure 3E). While BrdU incorporation can occur through both DNA repair and DNA replication, the amount of BrdU incorporated during those two events is very different, as DNA repair occurs in localized foci in the genome (37). The median fluorescence intensity (MFI) of BrdU⁺ TECs was more than 7 \times that of the whole cell population for both non-irradiated controls and day 7 postirradiation (Figure S4 in Supplementary Material), showing that BrdU incorporation after irradiation truly results from DNA replication. Also, BrdU MFI higher than that of BrdU⁺ TECs in the non-irradiated control (Figure S4 in Supplementary Material), suggesting that cells proliferating after irradiation went through more cycles of proliferation than those proliferating in steady-state. Interestingly, when compared with steady-state conditions (Figure 3A), the proportion of BrdU⁺ cells during post-SL-TBI regeneration showed conspicuous changes in two TEC subsets. First, the frequency of BrdU⁺ cells among UEA1⁺ NonLRCs (GFP⁻) was decreased by more than twofold (Figures 3E,F). Second, the salient finding was a conspicuous increase in the proportion of BrdU⁺UEA1⁻ LRCs which surpassed the proportion of BrdU⁺ elements in all other TEC subsets (Figures 3E,F). Overall, these results show that (i) UEA1⁺ NonLRCs are greatly affected by irradiation, resulting in cell death and decreased proliferation and (ii) that UEA1⁻ LRCs

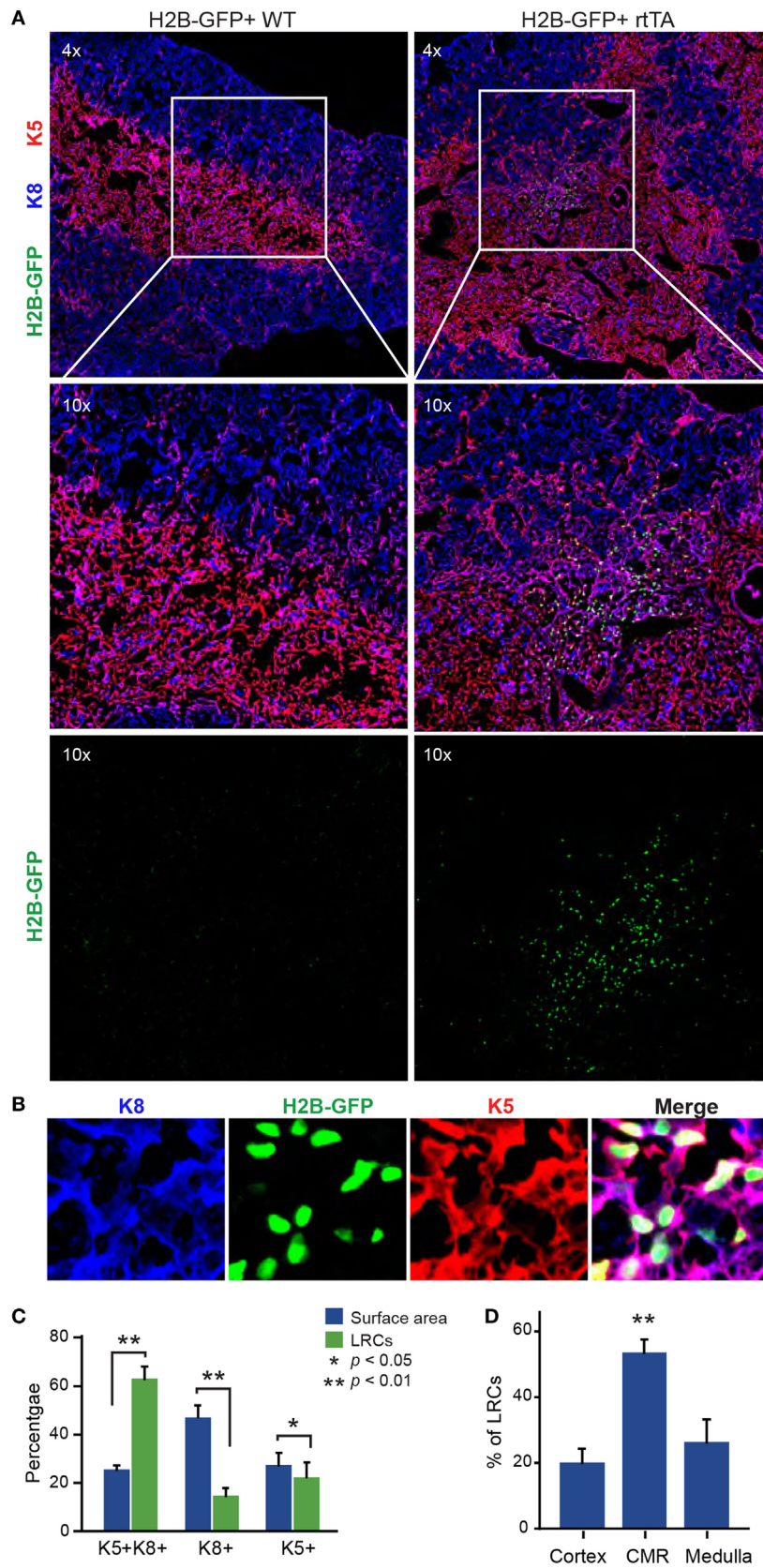


FIGURE 1 | Continued

FIGURE 1 | Continued

Most label-retaining cells (LRCs) are K5⁺K8⁺ and localized near the cortico-medullary junction. **(A)** Representative images of thymic slices after 16 weeks of chase in control (H2B-GFP⁺ WT, left panels) and test mice (H2B-GFP⁺ rTA, right panels). **(B)** Representative images of K5⁺K8⁺ GFP^{hi} cells. Cytokeratin K5 is shown in red, K8 in blue, and histone 2B-GFP fusion protein (H2B-GFP) in green. **(C)** Quantification of LRCs expressing K5, K8, or both cytokeratins. The number of LRCs per thymic lobe (green) from each TEC subset is compared with the surface area (blue) covered by this subset. **(D)** Percentage of LRCs found in different regions of the thymus. The proportions of LRCs are significantly higher in the cortico-medullary region (CMR) than the cortex or the medulla ($n = 4$).

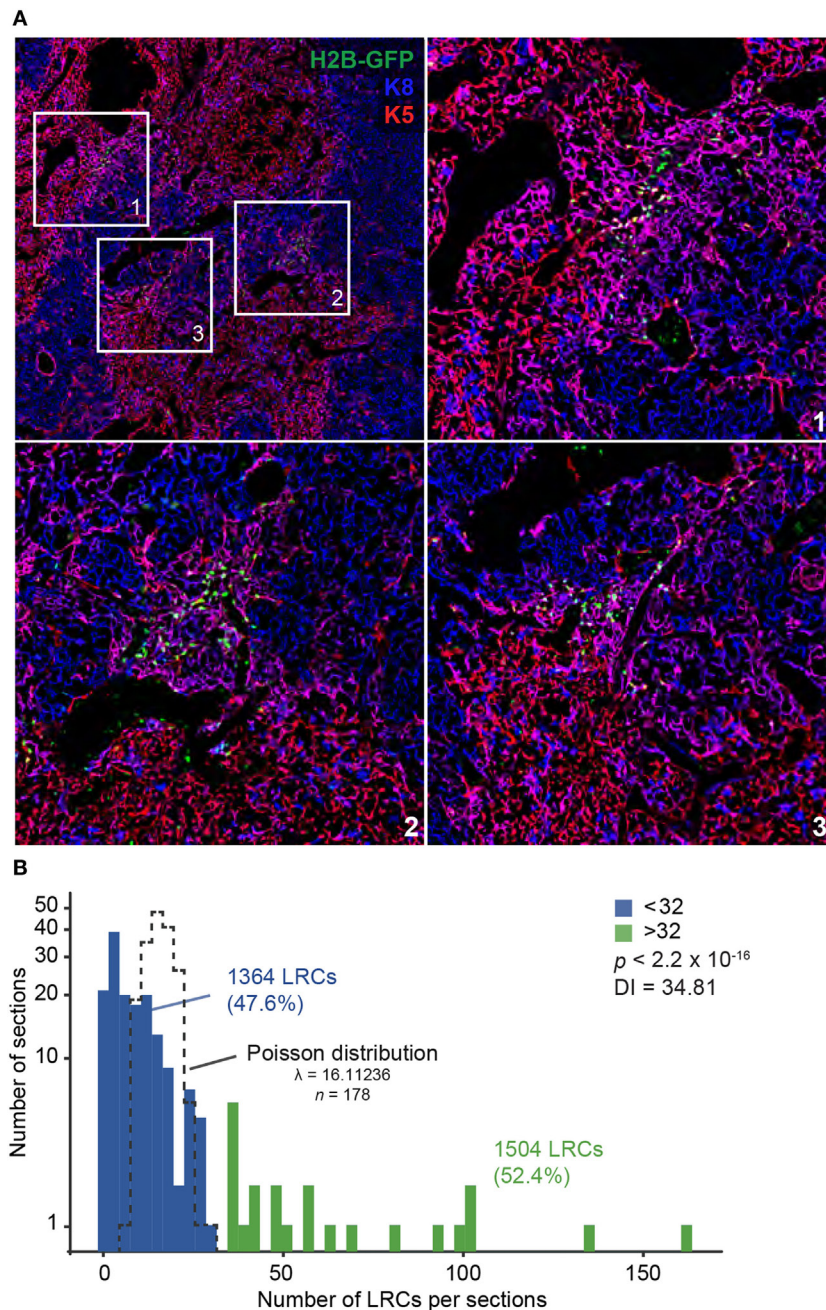
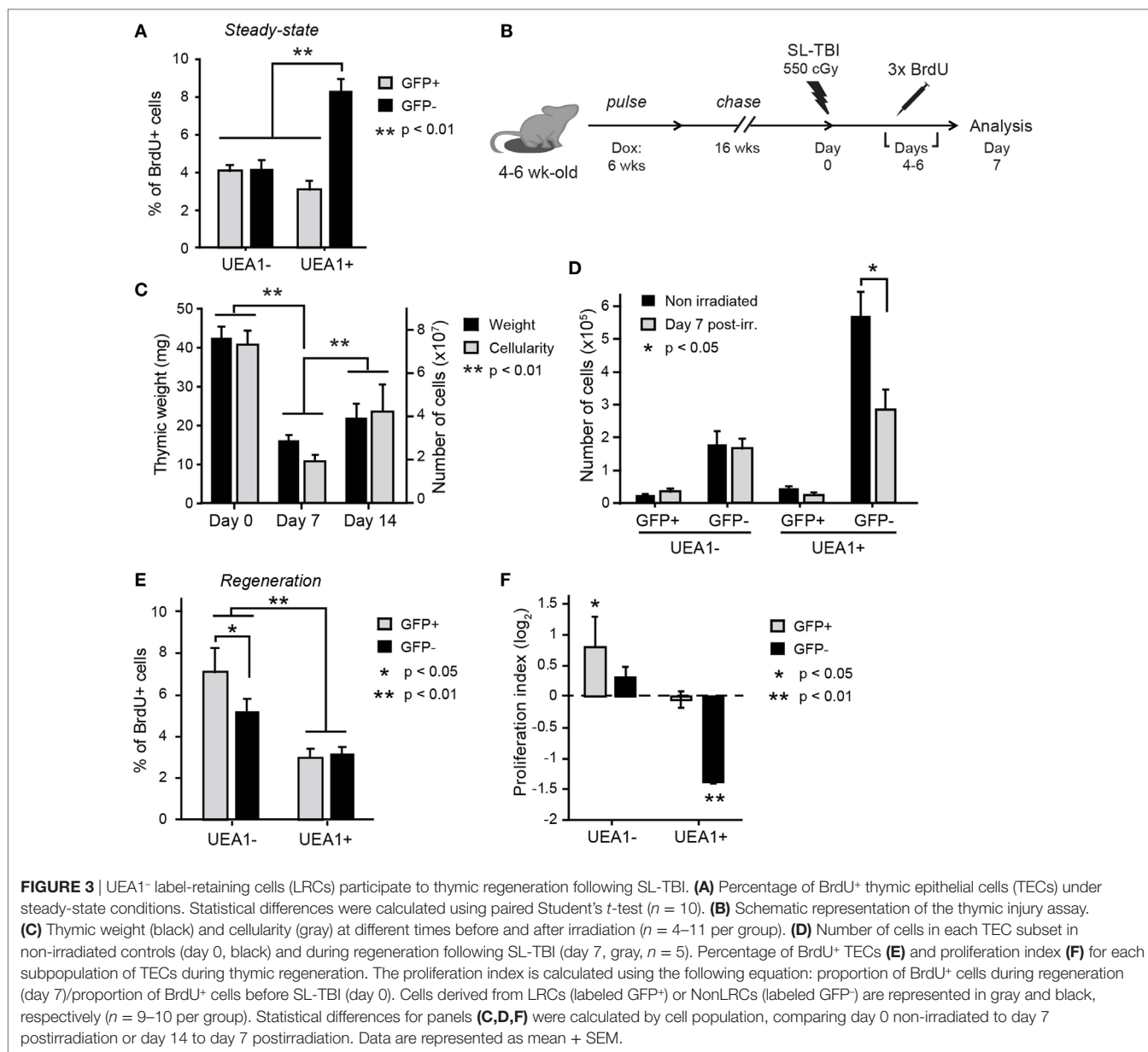


FIGURE 2 | Label-retaining cells (LRCs) are found in clusters at the cortico-medullary junction (CMJ). **(A)** Representative images of LRC clusters near the CMJ. Cytokeratin K5 is shown in red, K8 in blue, and H2B-GFP in green. **(B)** LRC distribution in the thymus. Each thymic slice was divided in 40–50 sections (see Figure S3B in Supplementary Material) for LRC quantification. Histogram shows the number of sections on the Y-axis (projected on a log scale) and the number of LRCs per section on the X-axis. The TEC distribution did not fit a Poisson distribution, shown with a black dotted line ($p < 2.2 \times 10^{-16}$; goodness of fit, maximum likelihood).



enrich for radioresistant TEPCs that actively proliferate during tissue regrowth.

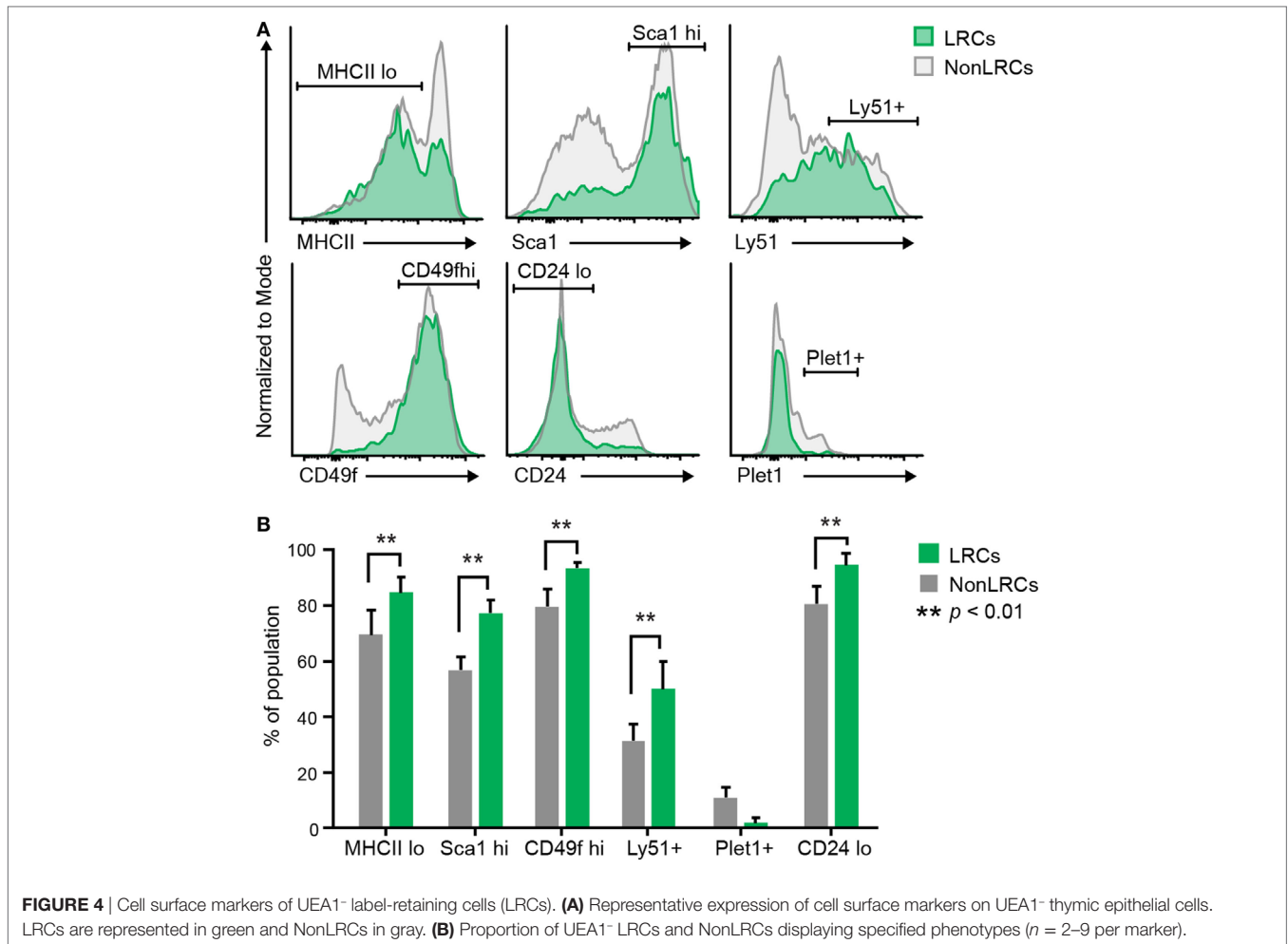
Cell Surface Phenotype of UEA1⁻ LRCs

Recent studies have reported the presence of bipotent TEPCs in the adult thymus. However, the cell surface phenotype of bipotent TEPCs in these three reports showed significant discrepancies (38–40). We therefore assessed whether UEA1⁻ LRCs expressed cell surface markers previously reported in bipotent TEPCs (Table S2 in Supplementary Material). When compared with UEA1⁻ NonLRCs, UEA1⁻ LRCs showed increased proportion of MHCII^{lo}, Sca1^{hi}, Cd49f^{hi}, and Ly51⁺ elements (Figure 4). Furthermore, UEA1⁻ LRCs were EpCAM⁺ (Figure S2 in Supplementary Material) and Plet1⁻ (Figure 4B). Therefore, the phenotype of UEA1⁻ LRCs is remarkably similar to that of

TEPCs reported by Wong et al. which were EpCAM⁺UEA1⁻MHCII^{lo}Sca1^{hi} and CD49f^{hi} Plet1⁻ (38).

Transcriptomic Analysis of UEA1⁻ LRCs and NonLRCs

To gain insights into the molecular and functional attributes of UEA1⁻ LRCs (enriched in radioresistant TEPCs), we compared their transcriptome to that of UEA1⁻ NonLRCs. To this end, we extracted and sequenced poly-A enriched mRNAs from sorted UEA1⁻ LRCs and NonLRCs using the Illumina HiSeq2000 platform. A total of 2,078 genes showed differential expression (fold change >2) between UEA1⁻ LRCs and NonLRCs, of which 1,450 (69.8%) were downregulated in UEA1⁻ LRCs (Table S3 in Supplementary Material). We then analyzed GO-term enrichment for each of the top 500 most differentially expressed genes.



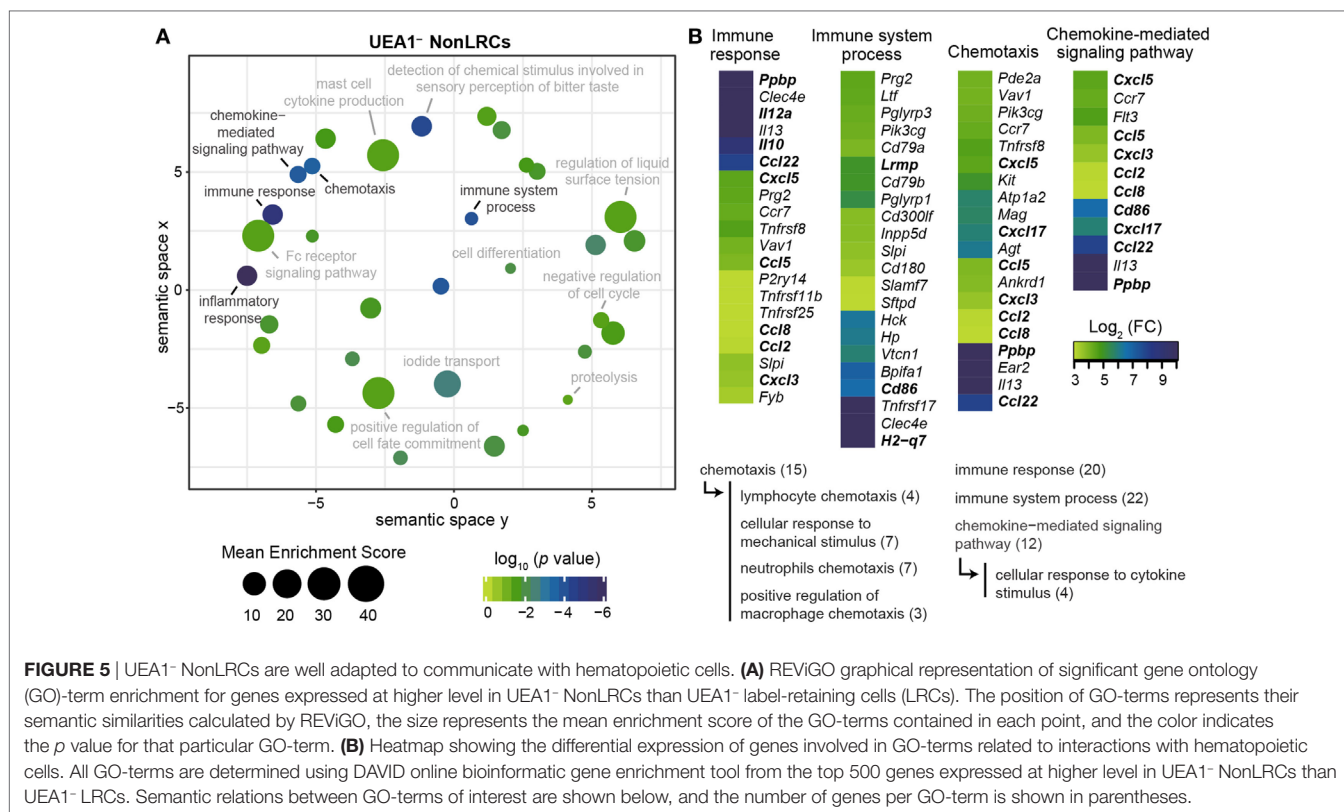
Using the gene-annotation enrichment tool DAVID (21, 22), we extracted GO-terms for each cell population and used the REVIGO software to reduce GO-terms redundancy.

Four GO-terms associated with the regulation of thymocytes maturation by TECs were significantly enriched in the gene set upregulated in UEA1⁻ NonLRCs (Figure 5). Notably, genes involved in antigen presentation (*Lrmp* and *H2-q7*) and thymocyte stimulation (*Cd86*, *Il10*, and *Il12a*) and chemotaxis (*Ccl22* and *Ppbbp*) were upregulated in NonLRCs (Figure 5B) (41–43). Moreover, many chemokines involved in the chemotaxis of dendritic cells and macrophages (*Ccl2*, *Ccl5*, *Ccl8*, *Cxcl3*, *Cxcl5*, and *Cxcl17*) were also upregulated in UEA1⁻ NonLRCs (44, 45). These results suggest that UEA1⁻ NonLRCs are better equipped than UEA1⁻ LRCs to interact with hematopoietic cells.

On the other hand, several genes upregulated in UEA1⁻ LRCs were associated with cell adhesion and cell migration (Figures 6A,B), including many secreted ECM proteins (*Col12a1*, *Col5a1*, *Fn1*, *Frem2*, *Lama4*, and *Sned1*) and molecules involved in cell–cell or cell–matrix adhesion (*Cldn5*, *Cdh5*, *Itga1*, *Itgb2*, *Sdk2*, *Tenm3*, and *Thbs1*). Contrary to UEA1⁻ NonLRCs, UEA1⁻ LRCs therefore seemed more adapted to interact with the surrounding stromal cells and ECM. Two genes specifically upregulated in

UEA1⁻ LRCs are involved in the regulation of stem cell activity in several tissues: *Podxl* and *Ptprz1* (Figure 6C). *Podxl*, a marker of cardiac, hematopoietic and mesenchymal stem cells, is involved in the maintenance of the immature state in cardiac stem cells and its downregulation facilitates their differentiation (46–48). *Ptprz1* is expressed in human embryonic stem cells and is downregulated during differentiation. While PTPRZ1 depletion is associated with a decrease in colony-formation potential of embryonic stem cells, its activation enhances the proliferation of embryonic stem cells (49). PTPRZ1 also negatively regulates oligodendrocyte precursor proliferation (50). Interestingly, the *Ptprz1* ligand *Ptn*, expressed by fibroblasts in the embryo, is also highly expressed by Sca1⁺ thymic mesenchymal cells (Figure 6C) but absent in TECs. The expression profile of *Ptprz1* (by UEA1⁻ LRCs) and *Ptn* (by Sca1⁺ mesenchymal cells) suggests that Sca1⁺ mesenchymal cells may be key components of the TEPC niche, as observed in other tissues (24). From these results, we conclude that *Podxl* and *Ptprz1* represent potential regulators of TEPC maintenance via interactions with stromal niche components.

Another GO-term significantly enriched in UEA1⁻ LRCs is directly related to stem cell regulation: *regulation of embryonic development* (Figures 6A,B). Two pathways associated with this



GO-term are also known to regulate thymopoiesis: androgen receptor and TGF- β . Androgen receptor is expressed by TECs and regulates their proliferation. Indeed, administration and ablation of androgen, respectively, lead to acute thymic involution and hypertrophy (6, 12, 13, 51). Of note, expression of androgen receptors by stromal cells is necessary for androgens to affect thymic cellularity (13, 51, 52). The fact that UEA1⁻ LRCs express higher levels of *Ar* transcripts than other types of thymic stromal cells (**Figure 6C**) suggests that the impact of androgens on thymopoiesis could be mediated primarily *via* regulation of TECs. In addition, TGF- β signaling in TECs was previously shown to decrease mTEC differentiation and maturation (53). Hence, though the precise role of TGFBR3 in TECs has not been elucidated, its higher expression in UEA1⁻ LRCs suggests that it might regulate their activity or differentiation (**Figure 6C**).

Typically, stem cells preferentially reside close to blood vessels in many tissues, including the bone marrow, hair follicle bulge and testes (54–56). Interestingly, the GO-term blood vessel development showed a very significant enrichment in UEA1⁻ LRCs ($p < 10^{-7}$, **Figures 6A,B**) and several genes overexpressed in UEA1⁻ LRCs regulate blood vessel stability (*Angpt1*, *Ptprb*, *C1galt1*, *Lama4*, *Mmrn2*, and *Flt1*). Interestingly, in addition to its implication in blood vessel development *Angpt1* is also involved in hematopoietic stem cell maintenance. Hematopoietic stem cells express high levels of ANGPT1, and TEK-ANGPT1 signaling facilitates adhesion of hematopoietic stem cells to their niche, increasing their stem cell activity (57). Of note, thymic Sca1⁺ mesenchymal cells also express high levels of *Tek*, the ligand for *Angpt1* (**Figure 6C**), suggesting that TEK-ANGPT1

interaction might also be involved in the maintenance of TEPCs. Finally, the WNT4 receptor *Fzd4* was expressed at higher levels in UEA1⁻ LRCs and Sca1⁺ mesenchymal cells compared with other stromal populations (**Figure 6C**). As WNT4 signaling enhances thymic cellularity through the expansion of TECs (58) and decreased WNT4 production contributes to thymic involution (59), expression of *Fzd4* by the TEPC-enriched population of UEA1⁻ LRCs and by Sca1⁺ mesenchymal cells suggests that WNT4 may regulate TEC maintenance primarily by regulating these two cell populations. Overall, our transcriptomic analyses suggest that while UEA1⁻ NonLRCs are specialized to communicate with hematolymphoid cells, UEA1⁻ LRCs interact mostly with the surrounding stromal cells and ECM. Furthermore, we have identified through transcriptomic sequencing six potential regulators of TEPCs (*Podxl*, *Ptprz1*, *Ar*, *Tgfb3*, *Angpt1*, and *Fzd4*) that are upregulated in UEA1⁻ LRCs.

DISCUSSION

In a previous study, we have demonstrated the presence of non-senescent LRCs in UEA1⁻ TECs (7). We now report that, together with their quiescent state, their resistance to radiations and their undifferentiated phenotype (K5⁺K8⁺) the ability of UEA1⁻ LRCs to participate to TEC regeneration after acute injury qualifies them as TEPCs. This conclusion is strengthened by two features of our experimental design. First, because of the constraints of the label-retention assay, our analyses on UEA1⁻ LRCs were performed in mice that were quite old, at 26–28 weeks of age. At this age, one would expect the global TEC population to have a

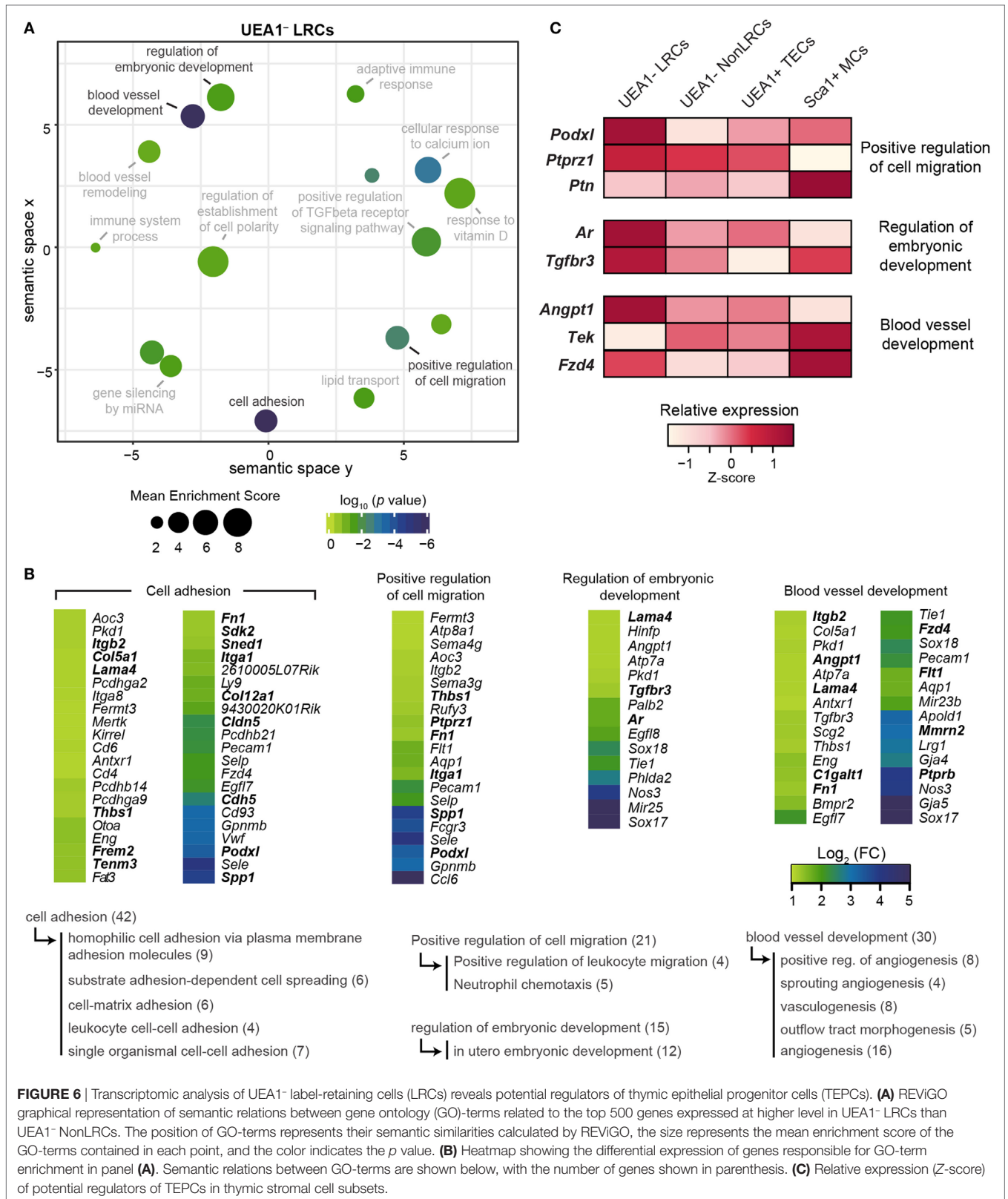


FIGURE 6 | Transcriptomic analysis of UEA1⁻ label-retaining cells (LRCs) reveals potential regulators of thymic epithelial progenitor cells (TEPCs). **(A)** REVI GO graphical representation of semantic relations between gene ontology (GO)-terms related to the top 500 genes expressed at higher level in UEA1⁻ LRCs than UEA1⁻ NonLRCs. The position of GO-terms represents their semantic similarities calculated by REVI GO, the size represents the mean enrichment score of the GO-terms contained in each point, and the color indicates the *p* value. **(B)** Heatmap showing the differential expression of genes responsible for GO-term enrichment in panel **(A)**. Semantic relations between GO-terms are shown below, with the number of genes shown in parenthesis. **(C)** Relative expression (Z-score) of potential regulators of TEPCs in thymic stromal cell subsets.

limited proliferation potential. Indeed, previous studies of TEPCs were performed either in newborns or in 6–8 weeks old mice (38–40). Second, we analyzed the proliferation of UEA1⁻ LRCs

in situ, without transplantation nor any *in vitro* purification step or culture. It has been shown that cells which are extracted from their normal environment and transplanted can acquire

stem cell properties that they do not display under steady-state conditions (19, 60). We therefore conclude that even in relatively old mice, UEA1⁻ LRCs have genuine TEPC activity after acute involution. During the regenerative phase following acute thymic injury induced by SL-TBI, UEA1⁻ LRCs were the most actively proliferating TEC subset. Interestingly, while the UEA1⁻ LRCs did not proliferate much under steady-state conditions, they increased their proliferation in the context of tissue repair. On the other hand, the TECs which proliferate most under steady-state conditions, i.e., UEA1⁺ NonLRCs, are the most affected by irradiation and barely proliferate during thymic regeneration. Of note, in addition to cell-intrinsic features (i.e., high percentage of cycling elements), the exquisite sensitivity of thymic UEA1⁺ NonLRCs to acute injury may be in part cell-extrinsic. Indeed, thymocyte-TEC cross talk is involved in thymic regeneration following total body irradiation (61). As irradiation leads to the depletion of thymocytes, it might disrupt interactions that allowed sustained proliferation and survival in mTECs. As UEA1⁻ LRCs express lower levels of genes involved in TEC-thymocyte interactions (Figure 6), they might be less dependent on cross talk with thymocytes. Our observations on TEC turnover are reminiscent of the intestinal epithelium, which possesses two types of stem cells: (i) rapidly cycling LGR5⁺ stem cell, responsible for steady-state maintenance of the intestinal epithelium and (ii) a pool of reserve quiescent stem cells that can compensate when the rapidly cycling LGR5⁺ stem cells are damaged (62). Our data suggest that UEA1⁻ LRCs are similar to the reserve quiescent stem cells in the intestinal epithelium. Likewise, other tissues including the cornea and the bone marrow contain quiescent stem cells that can be called upon in a context of injury (60, 62–64).

UEA1⁻ LRCs shared two features with the bipotent progenitors identified by Wong et al.: they display similar cell surface phenotypes and are both LRCs (38). This suggests that UEA1⁻ LRCs might contribute to the regeneration of both cTECs and mTECs following irradiation-induced injury. However, Ohigashi et al. reported that in adults, cTECs and mTECs were maintained by distinct progenitors, distinguished by their expression of the β 5T immunoproteasome subunit (65). Therefore, it is also possible that UEA1⁻ LRCs contribute only to the regeneration of cTECs. Our model unfortunately has limitations, inherent to the nature of the label-retention assay, which prevents us to fully explore these hypotheses. First, UEA1⁻ LRCs were enriched in TEPCs but they did not represent a pure TEPC population. Second, label-retention assays do not allow to perform *in situ* lineage tracing of LRCs to precisely characterize their differentiation potential. Pure quiescent TEPC populations and lineage tracing assays will be necessary to properly address these issues, which will require discovery and validation of new quiescent TEPC-specific markers.

Nevertheless, in addition to the identification of TEPCs in UEA1⁻ LRCs, our work (i) shows that most UEA1⁻ LRCs are found in clusters in the vicinity of the CMJ and (ii) presents a systems-level transcriptomic analysis of this TEPC-enriched cell subset. Moreover, RNA-Seq analyses revealed several interesting features of UEA1⁻ LRCs. Based on their transcriptome, UEA1⁻ NonLRCs would appear more qualified to interact with thymocytes whereas UEA1⁻ LRCs seem more adapted to interactions

with stromal cells and the ECM. These findings, together with evidence that UEA1⁻ LRCs are preferentially located in clusters in the CMR, suggest the existence of a specialized niche for TEPCs. More specifically, we identified three genes that may play a role in the regulation of TEPCs through interactions with niche cells: *Ptprz1*, *Podxl*, and *Angpt1*. In particular, the expression of the *Ptprz1* ligand *Ptn* by Sca1⁺ mesenchymal cells suggest that these cells are important components of the TEPC niche, as they are for the hematopoietic stem cell niche (24). Furthermore, many genes involved in blood vessel development were upregulated in UEA1⁻ LRCs compared with NonLRCs. This observation is coherent with the fact that blood vessels are crucial components of many types of stem/progenitor cell niches (66). Finally, among genes expressed at higher levels in UEA1⁻ LRCs than in UEA1⁻ NonLRCs, we identified three receptors whose ligands regulate TEC homeostasis: *Ar*, *Fzd4*, and *Tgfrb3*. Identification of these potential TEPC regulators warrants further investigation to better understand the mechanisms regulating the function of TEPCs and their interactions with niche cells. Investigations along these lines could provide evidence based strategies for enhancing TEC regeneration.

ETHICS STATEMENT

All procedures were in accordance with the Canadian Council on Animal Care guidelines and approved by the Comité de Déontologie et Expérimentation Animale de l'Université de Montréal.

AUTHOR CONTRIBUTIONS

MD-L: conception and design, collection, assembly, analysis, and interpretation of data, and manuscript writing. HG: conception and design, collection and assembly of data, and final revisions of the manuscript. TD, J-PL, SB, and SL: analysis and interpretation of data and final revisions of the manuscript. EG: conception and design and manuscript writing. CP: conception and design, provision of study material, financial support, and manuscript writing.

ACKNOWLEDGMENTS

The authors are grateful to Danielle Gagné and Gaël Dulude for flow cytometry and cell sorting, Jennifer Huber for RNA-sequencing experiments, and Isabelle Caron and Marie-Pierre Hardy for help with the thymic injury experiments and BrdU injections. Special thanks to Jarrod A. Dudakov for the insights on irradiation-induced thymic injury and for his advice on the design of this experiment.

FUNDING

This work was supported by grant FDN-148400 from the Canadian Institute of Health Research (CIHR). MDL is supported by a CIHR studentship and CP holds a Canada Research Chair in Immunobiology. The Institute for Research in Immunology and Cancer is supported in part by the Canada

Foundation for Innovation and the Fonds de la Recherche en Santé du Québec.

SUPPLEMENTARY MATERIAL

The Supplementary Material for this article can be found online at <http://www.frontiersin.org/article/10.3389/fimmu.2017.01717/full#supplementary-material>.

REFERENCES

- Blais M-É, Gérard G, Martinic MM, Roy-Proulx G, Zinkernagel RM, Perreault C. Do thymically and strictly extrathymically developing T cells generate similar immune responses? *Blood* (2004) 103:3102–10. doi:10.1182/blood-2003-09-3311
- Krueger A, Zięta N, Lyszkiwicz M. T cell development by the numbers. *Trends Immunol* (2017) 38:128–39. doi:10.1016/j.it.2016.10.007
- Breed ER, Lee ST, Hogquist KA. Directing T cell fate: how thymic antigen presenting cells coordinate thymocyte selection. *Semin Cell Dev Biol* (2017). doi:10.1016/j.semcdb.2017.07.045
- Anderson G, Takahama Y. Thymic epithelial cells: working class heroes for T cell development and repertoire selection. *Trends Immunol* (2012) 33:256–63. doi:10.1016/j.it.2012.03.005
- Bredenkamp N, Nowell CS, Blackburn CC. Regeneration of the aged thymus by a single transcription factor. *Development* (2014) 141:1627–37. doi:10.1242/dev.103614
- Gray DHD, Seach N, Ueno T, Milton MK, Liston A, Lew AM, et al. Developmental kinetics, turnover, and stimulatory capacity of thymic epithelial cells. *Blood* (2006) 108:3777–85. doi:10.1182/blood-2006-02-004531
- Dumont-Lagacé M, Brochu S, St-Pierre C, Perreault C. Adult thymic epithelium contains non-senescent label-retaining cells. *J Immunol* (2014) 192:2219–26. doi:10.4049/jimmunol.1302961
- Metzger TC, Khan IS, Gardner JM, Mouchess ML, Johannes KP, Krawisz AK, et al. Lineage tracing and cell ablation identify a post-Aire-expressing thymic epithelial cell population. *Cell Rep* (2013) 5:166–79. doi:10.1016/j.celrep.2013.08.038
- Chaudhry MS, Velardi E, Dudakov JA, van den Brink MRM. Thymus: the next (re)generation. *Immunol Rev* (2016) 271:56–71. doi:10.1111/immr.12418
- Dooley J, Liston A. Molecular control over thymic involution: from cytokines and microRNA to aging and adipose tissue. *Eur J Immunol* (2012) 42:1073–9. doi:10.1002/eji.201142305
- Dudakov JA, Hanash AM, Jenq RR, Young LF, Ghosh A, Singer NV, et al. Interleukin-22 drives endogenous thymic regeneration in mice. *Science* (2012) 336:91–5. doi:10.1126/science.1218004
- Griffith AV, Fallahi M, Venables T, Petrie HT. Persistent degenerative changes in thymic organ function revealed by an inducible model of organ regrowth. *Aging Cell* (2012) 11:169–77. doi:10.1111/j.1474-9726.2011.00773.x
- Velardi E, Tsai JJ, Holland AM, Wertheimer T, Yu VWC, Zakrzewski JL, et al. Sex steroid blockade enhances thymopoiesis by modulating Notch signaling. *J Exp Med* (2014) 211:2341–9. doi:10.1084/jem.20131289
- Chidgey A, Dudakov J, Seach N, Boyd R. Impact of niche aging on thymic regeneration and immune reconstitution. *Semin Immunol* (2007) 19:331–40. doi:10.1016/j.simm.2007.10.006
- Chung B, Barbara-Burnham L, Barsky L, Weinberg K. Radiosensitivity of thymic interleukin-7 production and thymopoiesis after bone marrow transplantation. *Blood* (2001) 98:1601–6. doi:10.1182/blood.V98.5.1601
- Weissman IL. Stem cells: units of development, units of regeneration, and units in evolution. *Cell* (2000) 100:157–68. doi:10.1016/S0092-8674(00)81692-X
- Fukada S, Uezumi A, Ikemoto M, Masuda S, Segawa M, Tanimura N, et al. Molecular signature of quiescent satellite cells in adult skeletal muscle. *Stem Cells* (2007) 25:2448–59. doi:10.1634/stemcells.2007-0019
- Tumbar T, Guasch G, Greco V, Blanpain C, Lowry WE, Rendl M, et al. Defining the epithelial stem cell niche in skin. *Science* (2004) 303:359–63. doi:10.1126/science.1092436
- Snippert HJ, Clevers H. Tracking adult stem cells. *EMBO Rep* (2011) 12:113–22. doi:10.1038/embor.2010.216
- Seach N, Wong K, Hammett M, Boyd RL, Chidgey AP. Purified enzymes improve isolation and characterization of the adult thymic epithelium. *J Immunol Methods* (2012) 385:23–34. doi:10.1016/j.jim.2012.07.023
- Huang DW, Sherman BT, Lempicki RA. Bioinformatics enrichment tools: paths toward the comprehensive functional analysis of large gene lists. *Nucleic Acids Res* (2009) 37:1–13. doi:10.1093/nar/gkn923
- Huang DW, Sherman BT, Lempicki RA. Systematic and integrative analysis of large gene lists using DAVID bioinformatics resources. *Nat Protoc* (2009) 4:44–57. doi:10.1038/nprot.2008.211
- Supek F, Bošnjak M, Škunca N, Šmuc T. REVIGO summarizes and visualizes long lists of gene ontology terms. *PLoS One* (2011) 6:e21800. doi:10.1371/journal.pone.0021800
- Patenaude J, Perreault C. Thymic mesenchymal cells have a distinct transcriptomic profile. *J Immunol* (2016) 196:4760–70. doi:10.4049/jimmunol.1502499
- Dumont-Lagacé M, St-Pierre C, Perreault C. Sex hormones have pervasive effects on thymic epithelial cells. *Sci Rep* (2015) 5:12895. doi:10.1038/srep12895
- Foudi A, Hochedlinger K, Van Buren D, Schindler JW, Jaenisch R, Carey V, et al. Analysis of histone 2B-GFP retention reveals slowly cycling hematopoietic stem cells. *Nat Biotechnol* (2009) 27:84–90. doi:10.1038/nbt.1517
- Fuchs E, Horsley V. Ferretting out stem cells from their niches. *Nat Cell Biol* (2011) 13:513–8. doi:10.1038/ncb0511-513
- Chakkalakal JV, Jones KM, Basson MA, Brack AS. The aged niche disrupts muscle stem cell quiescence. *Nature* (2012) 490:355–60. doi:10.1038/nature11438
- Rigamonti A, Brennand K, Lau F, Cowan CA. Rapid cellular turnover in adipose tissue. *PLoS One* (2011) 6:e17637. doi:10.1371/journal.pone.0017637
- Ohigashi I, Zuklys S, Sakata M, Mayer CE, Zhanybekova S, Murata S, et al. Aire-expressing thymic medullary epithelial cells originate from β 5t-expressing progenitor cells. *Proc Natl Acad Sci USA* (2013) 110:9885–90. doi:10.1073/pnas.1301799110
- Bleul CC, Corbeaux T, Reuter A, Fisch P, Mönning JS, Boehm T. Formation of a functional thymus initiated by a postnatal epithelial progenitor cell. *Nature* (2006) 441:992–6. doi:10.1038/nature04850
- Waghmare SK, Bansal R, Lee J, Zhang YV, McDermit DJ, Tumbar T. Quantitative proliferation dynamics and random chromosome segregation of hair follicle stem cells. *EMBO J* (2008) 27:1309–20. doi:10.1038/emboj.2008.72
- Rossi SW, Jenkinson WE, Anderson G, Jenkinson EJ. Clonal analysis reveals a common progenitor for thymic cortical and medullary epithelium. *Nature* (2006) 441:988–91. doi:10.1038/nature04813
- Pan B, Liu J, Zhang Y, Sun Y, Wu Q, Zhao K, et al. Acute ablation of DP thymocytes induces up-regulation of IL-22 and Foxn1 in TECs. *Clin Immunol* (2014) 150:101–8. doi:10.1016/j.clim.2013.11.002
- Popa I, Zubkova I, Medvedovic M, Romantseva T, Mostowski H, Boyd R, et al. Regeneration of the adult thymus is preceded by the expansion of K5+K8+ epithelial cell progenitors and by increased expression of Trp63, cMyc and Tcf3 transcription factors in the thymic stroma. *Int Immunol* (2007) 19:1249–60. doi:10.1093/intimm/dxm092
- Pawlik TM, Keyomarsi K. Role of cell cycle in mediating sensitivity to radiotherapy. *Int J Radiat Oncol Biol Phys* (2004) 59:928–42. doi:10.1016/j.ijrobp.2004.03.005
- Kao GD, McKenna WG, Yen TJ. Detection of repair activity during the DNA damage-induced G2 delay in human cancer cells. *Oncogene* (2001) 20:3486–96. doi:10.1038/sj.onc.1204445
- Wong K, Lister NL, Barsanti M, Lim JMC, Hammett MV, Khong DM, et al. Multilineage potential and self-renewal define an epithelial progenitor cell

- population in the adult thymus. *Cell Rep* (2014) 8:1198–209. doi:10.1016/j.celrep.2014.07.029
39. Ulyanchenko S, O'Neill KE, Medley T, Farley AM, Vaidya HJ, Cook AM, et al. Identification of a bipotent epithelial progenitor population in the adult thymus. *Cell Rep* (2016) 14:2819–32. doi:10.1016/j.celrep.2016.02.080
 40. Ucar A, Ucar O, Klug P, Matt S, Brunk F, Hofmann TG, et al. Adult thymus contains FoxN1⁺ epithelial stem cells that are bipotent for medullary and cortical thymic epithelial lineages. *Immunity* (2014) 41:257–69. doi:10.1016/j.immuni.2014.07.005
 41. Rodriguez-Galán MC, Bream JH, Farr A, Young HA. Synergistic effect of IL-2, IL-12, and IL-18 on thymocyte apoptosis and Th1/Th2 cytokine expression. *J Immunol* (2005) 174:2796–804. doi:10.4049/jimmunol.174.5.2796
 42. Snyder HL, Bacik I, Bennink JR, Kearns G, Behrens TW, Bächli T, et al. Two novel routes of transporter associated with antigen processing (TAP)-independent major histocompatibility complex class I antigen processing. *J Exp Med* (1997) 186:1087–98. doi:10.1084/jem.186.7.1087
 43. Tschöke SK, Oberholzer C, LaFace D, Hutchins B, Moldawer LL, Oberholzer A. Endogenous IL-10 regulates sepsis-induced thymic apoptosis and improves survival in septic IL-10 null mice. *Scand J Immunol* (2008) 68:565–71. doi:10.1111/j.1365-3083.2008.02176.x
 44. Chantry D, Romagnani P, Raport CJ, Wood CL, Epp A, Romagnani S, et al. Macrophage-derived chemokine is localized to thymic medullary epithelial cells and is a chemoattractant for CD3(+), CD4(+), CD8(low) thymocytes. *Blood* (1999) 94:1890–8.
 45. Fu WX, Gong SY, Qian XP, Li Y, Zhu ML, Dong XY, et al. Differential chemotactic potential of mouse platelet basic protein for thymocyte subsets. *Cell Mol Life Sci* (2004) 61:1935–45. doi:10.1007/s00018-004-4137-5
 46. Doyonnas R, Nielsen JS, Chelliah S, Drew E, Hara T, Miyajima A, et al. Podocalyxin is a CD34-related marker of murine hematopoietic stem cells and embryonic erythroid cells. *Blood* (2005) 105:4170–8. doi:10.1182/blood-2004-10-4077
 47. Lee RH, Seo MJ, Pulin AA, Gregory CA, Ylostalo J, Prockop DJ. The CD34-like protein PODXL and alpha6-integrin (CD49f) identify early progenitor MSCs with increased clonogenicity and migration to infarcted heart in mice. *Blood* (2009) 113:816–26. doi:10.1182/blood-2007-12-128702
 48. Moscoso I, Tejados N, Barreiro O, Sepúlveda P, Izarra A, Calvo E, et al. Podocalyxin-like protein 1 is a relevant marker for human c-kit(+) cardiac stem cells. *J Tissue Eng Regen Med* (2016) 10:580–90. doi:10.1002/term.1795
 49. Soh BS, Song CM, Vallier L, Li P, Choong C, Yeo BH, et al. Pleiotrophin enhances clonal growth and long-term expansion of human embryonic stem cells. *Stem Cells* (2007) 25:3029–37. doi:10.1634/stemcells.2007-0372
 50. Tamura H, Fukada M, Fujikawa A, Noda M. Protein tyrosine phosphatase receptor type Z is involved in hippocampus-dependent memory formation through dephosphorylation at Y1105 on p190 RhoGAP. *Neurosci Lett* (2006) 399:33–8. doi:10.1016/j.neulet.2006.01.045
 51. Olsen NJ, Olson G, Viselli SM, Gu X, Kovacs WJ. Androgen receptors in thymic epithelium modulate thymus size and thymocyte development. *Endocrinology* (2001) 142:1278–83. doi:10.1210/en.142.3.1278
 52. Lai K-P, Lai J-J, Chang P, Altuwajri S, Hsu J-W, Chuang K-H, et al. Targeting thymic epithelia AR enhances T-cell reconstitution and bone marrow transplant grafting efficacy. *Mol Endocrinol* (2013) 27:25–37. doi:10.1210/me.2012-1244
 53. Hauri-Hohl M, Zuklys S, Holländer GA, Ziegler SF. A regulatory role for TGF- β signaling in the establishment and function of the thymic medulla. *Nat Immunol* (2014) 15:554–61. doi:10.1038/ni.2869
 54. Boulais PE, Frenette PS. Making sense of hematopoietic stem cell niches. *Blood* (2015) 125:2621–9. doi:10.1182/blood-2014-09-570192
 55. Xiao Y, Woo W-M, Nagao K, Li W, Terunuma A, Mukoyama Y, et al. Perivascular hair follicle stem cells associate with a venule annulus. *J Invest Dermatol* (2013) 133:2324–31. doi:10.1038/jid.2013.167
 56. Yoshida S, Sukeno M, Nabeshima Y-I. A vasculature-associated niche for undifferentiated spermatogonia in the mouse testis. *Science* (2007) 317:1722–6. doi:10.1126/science.1144885
 57. Ikushima YM, Arai F, Nakamura Y, Hosokawa K, Kubota Y, Hirashima M, et al. Enhanced Angpt1/Tie2 signaling affects the differentiation and long-term repopulation ability of hematopoietic stem cells. *Biochem Biophys Res Commun* (2013) 430:20–5. doi:10.1016/j.bbrc.2012.11.002
 58. Heinonen KM, Vanegas JR, Brochu S, Shan J, Vainio SJ, Perreault C. Wnt4 regulates thymic cellularity through the expansion of thymic epithelial cells and early thymic progenitors. *Blood* (2011) 118:5163–73. doi:10.1182/blood-2011-04-350553
 59. Varcza Z, Kvell K, Talabér G, Miskei G, Csöngéi V, Bartis D, et al. Multiple suppression pathways of canonical Wnt signalling control thymic epithelial senescence. *Mech Ageing Dev* (2011) 132:249–56. doi:10.1016/j.mad.2011.04.007
 60. Sun J, Ramos A, Chapman B, Johnnidis JB, Le L, Ho Y-J, et al. Clonal dynamics of native haematopoiesis. *Nature* (2014) 514:322–7. doi:10.1038/nature13824
 61. Smith MJ, Reichenbach DK, Parker SL, Riddle MJ, Mitchell J, Osum KC, et al. T cell progenitor therapy-facilitated thymopoiesis depends upon thymic input and continued thymic microenvironment interaction. *JCI Insight* (2017) 2:92056. doi:10.1172/jci.insight.92056
 62. Tian H, Biehs B, Warming S, Leong KG, Rangell L, Klein OD, et al. A reserve stem cell population in small intestine renders Lgr5-positive cells dispensable. *Nature* (2011) 478:255–9. doi:10.1038/nature10408
 63. Nowell CS, Radtke F. Corneal epithelial stem cells and their niche at a glance. *J Cell Sci* (2017) 130:1021–5. doi:10.1242/jcs.198119
 64. Majo F, Rochat A, Nicolas M, Jaoudé GA, Barrandon Y. Oligopotent stem cells are distributed throughout the mammalian ocular surface. *Nature* (2008) 456:250–4. doi:10.1038/nature07406
 65. Ohigashi I, Zuklys S, Sakata M, Mayer CE, Hamazaki Y, Minato N, et al. Adult thymic medullary epithelium is maintained and regenerated by lineage-restricted cells rather than bipotent progenitors. *Cell Rep* (2015) 13:1432–43. doi:10.1016/j.celrep.2015.10.012
 66. Mendelson A, Frenette PS. Hematopoietic stem cell niche maintenance during homeostasis and regeneration. *Nat Med* (2014) 20:833–46. doi:10.1038/nm.3647

Conflict of Interest Statement: The authors declare that the research was conducted in the absence of any commercial or financial relationships that could be construed as a potential conflict of interest.

Copyright © 2017 Dumont-Lagacé, Gerbe, Daouda, Laverdure, Brochu, Lemieux, Gagnon and Perreault. This is an open-access article distributed under the terms of the Creative Commons Attribution License (CC BY). The use, distribution or reproduction in other forums is permitted, provided the original author(s) or licensor are credited and that the original publication in this journal is cited, in accordance with accepted academic practice. No use, distribution or reproduction is permitted which does not comply with these terms.